

## Ellipsometric investigation of metal-alkali-halide interfaces

V. M. Bermudez

Naval Research Laboratory, Washington, D.C. 20375

(Received 31 August 1984)

Spectroscopic ellipsometry ( $1.5 < h\nu < 5.0$  eV) has been used to follow the evolution of the complex optical dielectric function of Al, Cu, and Pt films with increasing coverage on the (100) surfaces of KCl and NaCl cleaved in ultrahigh vacuum. At low coverages, optical absorptions are observed which are not present in the bulk metal or dielectric. The results can be accounted for in terms of an effective-medium mixture of metal particles in a dielectric host. No optical transitions related to either interface states or defects were detected.

Because of their technological importance, metal/semiconductor interfaces have been studied extensively<sup>1</sup> using the full array of surface-sensitive electron spectroscopies. Recently, attention has been directed to metal/oxide (e.g., Pt/TiO<sub>2</sub>, Al/SiO<sub>2</sub>) interfaces as a result of their relevance to catalysis<sup>2</sup> and to metal-oxide semiconductor (MOS) structures.<sup>3</sup>

By contrast, little work has been carried out on interfaces between metals and alkali halides or alkaline-earth fluorides. It is anticipated that heterostructures involving these wide-band-gap insulators will become more important as their application in semiconductor passivation increases.<sup>4,5</sup> Recently, calculations have been performed<sup>6</sup> in which the Schottky barrier heights for metal/BaF<sub>2</sub> and metal/LiF interfaces were derived in terms of the band parameters of the metal and insulator. The results are in excellent agreement with experiment.<sup>7</sup> Also, Ernst<sup>8</sup> has estimated the work functions of single-crystal NaCl and KCl by measuring the photoelectron yield curve of electrons transferred to these materials by contact with metals of different work function.

The halide materials are very difficult to study by conventional techniques of surface science (e.g., photoemission and Auger spectroscopies) because of specimen charging effects<sup>9</sup> and the rapid decomposition of the substrate during electron bombardment, even at small current densities.<sup>10,11</sup> These problems can be circumvented by an entirely optical technique, such as Raman spectroscopy<sup>5</sup> or ellipsometry.

In this work we have used spectroscopic ellipsometry from the near infrared to the near ultraviolet (uv) to investigate the interaction between ultrahigh vacuum (UHV)-cleaved (100) surfaces of KCl and NaCl and submonolayer coverages of Al, Cu, and Pt deposited by *in situ* evaporation. Particular attention is given to the possible formation of interface states,<sup>6</sup> including point defects (color centers) in the substrate. Previously,<sup>12</sup> ellipsometry has been employed to obtain the optical spectrum of *F* centers (an electron trapped at a Cl<sup>-</sup> vacancy) formed on the surface of KCl by vacuum-ultraviolet irradiation. Spectra have been obtained from coverages near the detection limit up to coverages at which the bulk metallic features begin to emerge. Because of the strong dependence of the film optical properties on morphology,<sup>13,14</sup> we have concentrated primarily on unusual features in the spectra obtained at the earliest stages of film formation.

The optical instrumentation is a more highly automated version of the polarization modulation ellipsometer described in Refs. 12 and 15. Here we will briefly describe

only the refinements to the basic instrument. The system is now controlled by a microcomputer (64K Apple II+) which steps the double monochromator, sets the modulation amplitude, averages repeated readings of the outputs of both lock-in amplifiers (tuned to the first and second harmonics of the modulation frequency), and plots the raw data. The computer calculates the correct modulation amplitude control voltage, which is a nonlinear function of the wavelength  $\lambda$ , using the coefficients of a previously determined polynomial and then generates the voltage using a 12-bit digital-to-analog converter. As described previously,<sup>15</sup> calibration of the first-harmonic (*f*) signal requires a broadband achromatic  $\lambda/4$  plate. This is now accomplished by using the output of the  $2f$  lock-in (which should be identically zero under the conditions of the *f* calibration) as an error signal to drive a Babinet-Soleil compensator *via* a servomotor. At the end of the experiment, the accumulated raw data are transferred over a telephone line to a main-frame computer for further analysis and plotting.

All experiments were performed in a conventional stainless steel UHV chamber with a base pressure below  $3 \times 10^{-10}$  Torr. Single-crystal blocks (approximately  $10 \times 15 \times 25$  mm<sup>3</sup>) of KCl and NaCl were securely mounted in a hollow Al block by potting with In metal, leaving half of the 25-mm length projecting outward. The rear surface ( $10 \times 15$  mm<sup>2</sup>) was coated with colloidal graphite (Aquadag) before mounting to reduce the effects of back-surface reflections. The length of the sample further ensured that such extraneous reflections were well displaced from the front-surface specular beam. Cleaving was performed using an opposing knife-edge and anvil assembly. The evaporation sources consisted of high purity Cu, Al, and Pt wires wrapped on tungsten filaments and were thoroughly outgassed before cleaving the samples. The chamber pressure rose to, at most, the upper  $10^{-9}$ -Torr range during evaporation then returned quickly to the base pressure. The sample was nominally at room temperature during deposition and was not annealed afterwards. The angle of incidence was 61.7°, chosen close to the Brewster angle to maximize sensitivity to very thin surface films. Experiments consisted of measuring the ellipsometric angles  $\psi$  and  $\Delta$  vs  $\lambda$  for the freshly cleaved surface and for the same surface after successive metal depositions. Two-zone averaging<sup>16,17</sup> was used to reduce the effects of systematic errors, and a further correction was applied for the small birefringence of the entrance window. The dielectric function ( $\tilde{\epsilon} = \epsilon_1 + i\epsilon_2$ ) of the surface film was determined from these data using the itera-

tive procedure described previously.<sup>12</sup>  $\psi$  and  $\Delta$  were also monitored, at fixed  $\lambda$ , during film growth by tuning the monochromator to  $\lambda = 300.6$  nm and placing a uv bandpass filter (Corning 7-54) in front of the detector to block light from the evaporation filament. For the case of Pt, which requires high evaporation temperatures, this technique was only partly successful.

Figure 1 summarizes the experimental results for Cu on KCl. First, the inset shows the  $\Delta$  vs  $\psi$  plot obtained during successive depositions (points) and that calculated for a bulk-Cu layer. The fixed- $\lambda$  measurements were not corrected for small systematic errors; hence, the clean-surface value of  $\Delta$  is not exactly zero. The calculated  $\psi$  and  $\Delta$  are strong functions of the thickness up to a few hundred angstroms, beyond which (at  $\lambda = 300$  nm) the optical path length of the specular beam through the film significantly exceeds the optical attenuation length. The calculated curve follows the experimental points reasonably well up to  $\sim 50$  Å. However, the thickness values along the calculated curve cannot be interpreted as the "true" layer thickness since analysis of the spectra (discussed below), as well as previous work<sup>19</sup> on the growth of very thin metal films on alkali halides at room temperature, indicates that the films

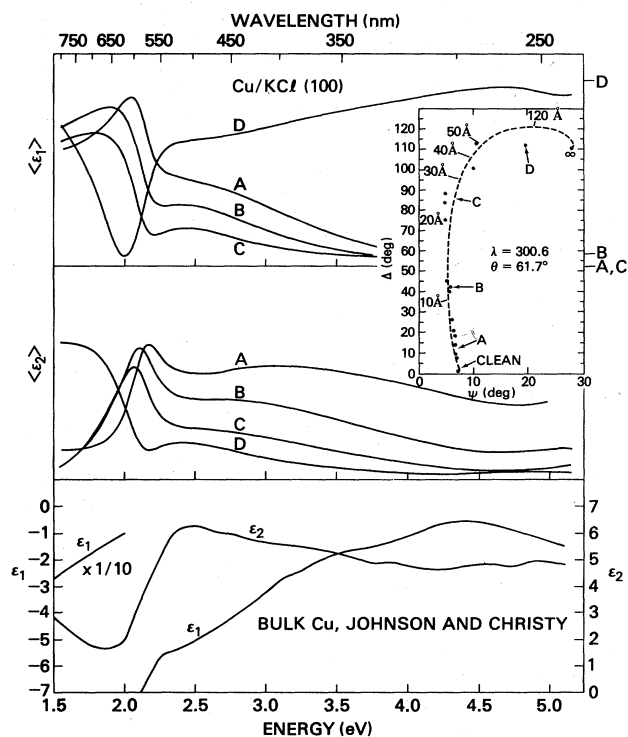


FIG. 1. Real ( $\langle \epsilon_1 \rangle$ ) and imaginary ( $\langle \epsilon_2 \rangle$ ) effective dielectric functions of Cu/KCl for increasing deposition and for bulk Cu (Ref. 18). The absolute values of  $\langle \epsilon_1 \rangle$  and  $\langle \epsilon_2 \rangle$  are indeterminate (see text). The labels A, B, etc., on the right-hand axis of the  $\langle \epsilon_1 \rangle$  plot give the respective zero levels. The inset shows the  $\psi, \Delta$  plot at  $61.7^\circ$  angle of incidence and  $\lambda = 300.6$  nm. The dashed curve was calculated (as a function of film thickness, indicated in angstroms at several points on the curve) using the bulk Cu optical constants (Ref. 18). The solid points are the experimental quantities, and the labels A, B, etc., indicate the stages during deposition at which the spectra were obtained.

form discontinuously, as islands. Hence, the model thickness represents that of an equivalent homogeneous film for which the calculated  $\psi$  and  $\Delta$  would agree with those observed for the real film, if the model film were optically equivalent to bulk Cu at the specified  $\lambda$ . The model is only qualitative, as shown by the deviation of the calculation from experiment at higher coverages where  $\psi$  and  $\Delta$  are both changing. The utility of the  $\psi, \Delta$  plot is that it provides some measure of the difference in surface coverage at the indicated points (A–D) during growth at which spectra were obtained.

Figure 1 shows the "effective dielectric function" ( $\langle \tilde{\epsilon} \rangle$ ), at different coverages. The term "effective" means that all changes in the surface induced by metal deposition, including island formation and any structural changes in the substrate itself, are modeled in terms of a single homogeneous and isotropic layer. The spectra show that  $\langle \tilde{\epsilon} \rangle$  differs considerably from that of bulk Cu. At some point between C and D, the film does become metallic (i.e.,  $\langle \epsilon_1 \rangle < 0$ ); although the Drude region below  $\sim 2$  eV may still be affected by the finite particle size.<sup>13,14</sup> Since the value of the film thickness used in the numerical inversion of the Fresnel relations<sup>12</sup> is arbitrary, the absolute magnitude of  $\langle \tilde{\epsilon} \rangle$  is indeterminate. Large changes (factors of 2 or 3) in the value used had only small effects on the overall shapes of the spectra, mainly toward the uv end.

Figure 2 shows  $\langle \epsilon_2 \rangle$  for thin films of Al, Cu, and Pt on KCl. The Cu curve is the same as that labeled "A" in Fig. 1. Similar results were obtained for Cu and Pt on NaCl; Al/NaCl was not studied. With increasing thickness, the broad maxima in the Al and Pt spectra shift to lower energy and broaden until the bulk  $\tilde{\epsilon}$  begins to emerge at higher coverage. Neither Al (Ref. 20) nor Pt (Ref. 21) have any structure in the bulk  $\epsilon_2$  comparable to that shown in Fig. 2.

To account for these results, calculations were performed based on the Bruggemann effective-medium approximation<sup>13</sup> (EMA) in which the surface layer is modeled as metal-filled voids (with dielectric function  $\tilde{\epsilon}_v$  equal to that of the bulk metal) in a host matrix (with  $\tilde{\epsilon}_h$  equal to that of the alkali halide). The results obtained using  $\tilde{\epsilon}_h$  given by Li (Ref. 22) and  $\tilde{\epsilon}_v$  from the recent tabulation by Palik<sup>23</sup> are shown in Fig. 3. For Cu, the coverage-dependent  $\langle \epsilon_2 \rangle$  in Fig. 1 are quite well reproduced by the calculation, with the void fraction  $f_v$  as the only adjustable parameter. In particular, the peak appearing at  $\sim 2.2$  eV at lowest coverage shifts to lower energy and gains intensity, relative to the interband spectrum ( $> 2.5$  eV) with increasing coverage.

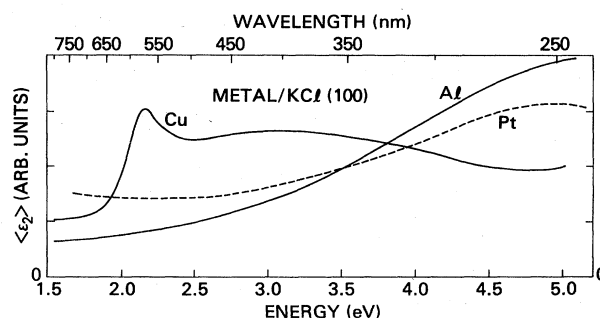


FIG. 2. Imaginary effective dielectric functions ( $\langle \epsilon_2 \rangle$ ) for very small coverages of Cu, Al, and Pt on KCl.

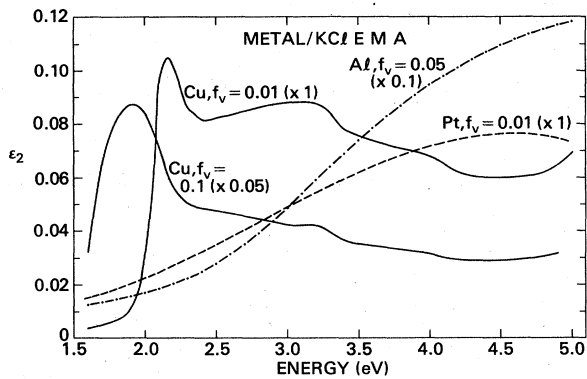


FIG. 3. Calculated  $\epsilon_2$  for discontinuous metal films on KCl. The void fractions  $f_v$  used in the effective-medium approximation and the relative scale factors (in parenthesis) are indicated.

The structure in  $\tilde{\epsilon}$  is very sensitive to the value of  $f_v$ , as shown by the Cu results, and the energy of the broad maxima in the Pt and Al results can be shifted significantly by small adjustments of the assumed void fraction.

The choice of  $\tilde{\epsilon}_v$  is justified by theoretical<sup>24</sup> (Al and Cu) and experimental<sup>25</sup> (Cu) work indicating that clusters containing only a few atoms begin to show rudimentary band structure which quickly converges to that of the bulk with increasing cluster size. For comparison, calculations were also done for Cu with  $\tilde{\epsilon}_h = 1$  (vacuum as the host dielectric); these give  $\epsilon_2$  qualitatively similar to those in Fig. 3 but with the structure above 2.5 eV more pronounced than the  $\sim 2.2$ -eV peak. Finally, the shapes of the calculated  $\epsilon_1$  curves were also in reasonable agreement with experiment except for Cu below 2.5 eV, where the Drude contribution is large. Since the void sizes and shapes are not well characterized, no attempt has been made to account for the effect of finite particle dimensions<sup>13,14</sup> on the Drude function (which may be more significant for the Cu than for the Pt

and Al films).

No additional structure was observed, such as might be associated with optical excitation within the Schottky barrier, the height of which can be estimated using the results in Ref. 6. Furthermore, no evidence of the KCl  $F$  center (2.2 eV) or the  $M$  center ( $F$  center dimer, 1.5 eV) absorption bands was observed. Based on previous work,<sup>12</sup> the detection limit is estimated to be about  $3 \times 10^{12}$   $F$  centers/cm<sup>2</sup>.

The purpose of this work is an investigation of the application of spectroscopic ellipsometry to understanding the electronic structure of metal-alkali-halide interfaces (and, by implication, of other similar heterostructures). Although a large number of optical studies has been carried out on metal films (Refs. 13, 14, 23, and works cited), most of these have focused on layers of several tens of angstroms or more in equivalent thickness. The present experiments have been concerned with the interband region at the early stages of film growth. The results indicate that the spectra are dominated by optical excitations of small metal islands imbedded in a dielectric matrix. As noted above, the results in Fig. 3 are not very sensitive to the choice of  $\tilde{\epsilon}_h$  (i.e., vacuum or KCl). Hence, the optical data do not provide detailed information about the location of the metal islands on the surface. However, the somewhat better agreement obtained for  $\tilde{\epsilon}_h$  equal to that of KCl suggests that island formation occurs at cleavage-induced surface irregularities (such as steps) rather than on smooth flat areas.

For more reactive interfaces, such as transition metals on Si, one would expect additional structure in the spectra resulting from compound (e.g., silicide) formation as well as from adsorption-induced changes in the surface dielectric function of the substrate.<sup>26</sup> However, any optical study of such metal/substrate interfaces will be complicated by the effects observed here if heterogeneous film formation occurs. Recent ellipsometric work<sup>27</sup> on the interface between Al and a Si (111) surface, prepared by flashing in UHV to 1100°C prior to Al deposition, suggests island growth phenomena similar to those reported here.

<sup>1</sup>L. J. Brillson, *J. Phys. Chem. Solids* **44**, 703 (1983); *Surf. Sci. Rep.* **2**, 123 (1982).

<sup>2</sup>S. J. Tauster, S. C. Fung, R. T. K. Baker, and J. A. Horsley, *Science* **211**, 1121 (1981).

<sup>3</sup>R. S. Bauer, R. Z. Bachrach, and L. J. Brillson, *Appl. Phys. Lett.* **37**, 1006 (1980).

<sup>4</sup>J. M. Phillips, L. C. Feldman, J. M. Gibson, and M. L. McDonald, *Thin Solid Films* **104**, 101 (1983); B. W. Sloope, *J. Vac. Sci. Technol. A* **1**, 564 (1983).

<sup>5</sup>M. B. Stern, T. R. Harrison, V. D. Archer, P. F. Liao, and J. C. Bean, *Solid State Commun.* **51**, 221 (1984).

<sup>6</sup>T. E. Feuchtwang, D. Paudyal, and W. Pong, *Phys. Rev. B* **26**, 1608 (1982).

<sup>7</sup>W. Pong and D. Paudyal, *Phys. Rev. B* **23**, 3085 (1981).

<sup>8</sup>L. Ernst, *Solid State Commun.* **19**, 311 (1976).

<sup>9</sup>R. T. Williams, D. J. Nagel, and M. N. Kabler, *J. Phys. (Paris) Colloq.* **41**, C6-439 (1980).

<sup>10</sup>C. L. Strecker, W. E. Moddeman, and J. T. Grant, *J. Appl. Phys.* **52**, 6921 (1981).

<sup>11</sup>A. Friedenbergl and Y. Shapira, *Surf. Sci.* **87**, 581 (1979).

<sup>12</sup>V. M. Bermudez, *Surf. Sci.* **74**, 568 (1978); **94**, 29 (1980).

<sup>13</sup>O. Hunderi, *Thin Solid Films* **57**, 15 (1979); *Surf. Sci.* **96**, 1 (1980).

<sup>14</sup>D. E. Aspnes, E. Kinsbron, and D. D. Bacon, *Phys. Rev. B* **21**, 3290 (1980).

<sup>15</sup>V. M. Bermudez and V. H. Ritz, *Appl. Opt.* **17**, 548 (1978).

<sup>16</sup>V. M. Bermudez, *Opt. Commun.* **23**, 413 (1977); **24**, 366(E) (1978).

<sup>17</sup>F. A. Modine, G. E. Jellison, Jr., and G. R. Gruzalski, *J. Opt. Soc. Am.* **73**, 892 (1983).

<sup>18</sup>P. B. Johnson and R. W. Christy, *Phys. Rev. B* **6**, 4370 (1972).

<sup>19</sup>J. Metois, M. Gauch, A. Masson, and R. Kern, *Thin Solid Films* **11**, 205 (1972).

<sup>20</sup>E. Shiles, T. Sasaki, M. Inokuti, and D. Y. Smith, *Phys. Rev. B* **22**, 1612 (1980).

<sup>21</sup>J. H. Weaver, *Phys. Rev. B* **11**, 1416 (1975).

<sup>22</sup>H. H. Li, *J. Phys. Chem. Ref. Data* **5**, 329 (1976).

<sup>23</sup>E. D. Palik, *Handbook of Optical Constants* (Academic, New York, in press).

<sup>24</sup>R. P. Messmer, S. K. Knudson, K. H. Johnson, J. B. Diamond, and C. Y. Yang, *Phys. Rev. B* **13**, 1396 (1976); D. R. Salahub and R. P. Messmer, *ibid.* **16**, 2526 (1977).

<sup>25</sup>M. Moskovits and J. E. Hulse, *J. Chem. Phys.* **67**, 4271 (1977).

<sup>26</sup>V. M. Bermudez and V. H. Ritz, *Phys. Rev. B* **26**, 3297 (1982).

<sup>27</sup>V. M. Bermudez (unpublished).